Inorg. Chem. **2008**, *47*, 1639−1647

Kinetics and Mechanisms of Chlorine Dioxide Oxidation of Tryptophan

David J. Stewart, **Michael J. Napolitano**, **Ekaterina V. Bakhmutova-Albert**, **and Dale W. Margerum***

Department of Chemistry, Purdue University, West Lafayette, Indiana 47907-2084

Received September 7, 2007

The reactions of aqueous $ClO_2^{\bullet}$ and tryptophan (Trp) are investigated by stopped-flow kinetics, and the products are identified by high-performance liquid chromatography (HPLC) coupled with electrospray ionization mass spectrometry and by ion chromatography. The rates of $ClO_2^{\bullet}$ loss increase from pH 3 to 5, are essentially constant from pH 5 to 7, and increase from pH 7 to 10. The reactions are first-order in Trp with variable order in $ClO_2^{\bullet}$. Below pH 5.0, the reactions are second- or mixed-order in [$ClO_2^{\bullet}$], depending on the chlorite concentration. Above pH 5.0, the reactions are first-order in [$ClO_2^{\bullet}$] in the absence of added chlorite. At pH 7.0, the Trp reaction with $ClO_2^{\bullet}$ is first-order in each reactant with a second-order rate constant of 3.4×10^4 M^{-1} s^{-1} at 25.0 °C. In the proposed mechanism, the initial reaction is a one-electron oxidation to form a tryptophyl radical cation and chlorite ion. The radical cation deprotonates to form a neutral tryptophyl radical that combines rapidly with a second $ClO_2^{\bullet}$ to give an observable, short-lived adduct ($k_{obs} = 48$ s^{-1}) with proposed C(H)−OClO bonding. This adduct decays to give HOCl in a three-electron oxidation. The overall reaction consumes two $ClO_2^{\bullet}$ per Trp and forms ClO_2^- and HOCl. This corresponds to a four-electron oxidation. Decay of the tryptophyl−OClO adduct at pH 6.4 gives five initial products that are observed after 2 min and are separated by HPLC with elution times that vary from 4 to 17 min (with an eluent of 6.3% CH_3OH and 0.1% CH_3COOH). Each of these products is characterized by mass spectrometry and UV–vis spectroscopy. One initial product with a molecular weight of 236 decays within 47 min to yield the most stable product, *N*-formylkynurenine (NFK), which also has a molecular weight of 236. Other products also are observed and examined.

Introduction

Aqueous $ClO_2^{\bullet}$ has been used to purify water,[1,2] while gaseous $ClO_2^{\bullet}$ has been used in chemosterilization[3] and disinfection of anthrax.[4] Aqueous $ClO_2^{\bullet}$ has seen an increased role as a sanitizing agent in the food industry, including vegetable processing,[5–7] citrus packing,[8] fish,[9–11] meat,[12] and poultry processing.[13,14] Because of the increased use of $ClO_2^{\bullet}$ as a disinfecting agent, the most reactive amino acids and other biological molecules are targets of great interest to determine its behavior. The kinetics and mechanism of tyrosine,[15] cysteine,[16] and 5′-guanosine monosphosphate[17] have recently been examined in their reactions with $ClO_2^{\bullet}$.

Other studies of the oxidation of tryptophan (Trp) have been performed in several different ways, including photooxidation,[18–24] the use of peroxy-type reactants,[25–27] elec-

* To whom correspondence should be addressed. E-mail: margerum@purdue.edu.

(1) Katz, A.; Narkis, N. *Water Res.* **2001**, *35*, 101–108.
(2) Elphick, A. *Processing (Sutton, Engl.)* **1998**, *34*, 122–125.
(3) Rosenblatt, D. H. U.S. Patent 4,504,442, 1983.
(4) Ritter, S. K. *Chem. Eng. News* **2001**, *79*, 24–26.
(5) Costilow, R. N.; Uebersax, M. A.; Ward, P. J. *J. Food Sci.* **1984**, *49*, 396–401.
(6) Reina, L. D.; Fleming, H. P.; Humphries, E. G. *J. Food Prot.* **1995**, *58*, 541–546.
(7) Zhang, S.; Farber, J. M. *Food Microbiol.* **1996**, *13*, 311–321.
(8) Brown, G. E.; Wardowski, W. F. *Citrus Ind.* **1986**, *67*, 48–56.
(9) Key, A. M.; Grodner, R. M.; Park, D. L.; Luizo, J.; Kilgen, M. L.; Andrews, L. S. *IFT annual meeting: book of abstracts*;Dekker: New York, 1996; p 133.
(10) Lin, W. F.; Huang, T. S.; Cornell, J. A.; Lin, C. M.; Wei, C. I. *J. Food Sci.* **1996**, *61*, 1030–1034.
(11) Kim, J. M.; Huang, T. S.; Marshall, M. R.; Wei, C. I. *J. Food Sci.* **1999**, *64*, 1089–1093.
(12) Cutter, C. N.; Dorsa, W. J. *J. Food Prot.* **1995**, *58*, 1294–1296.
(13) Villarreal, M. E.; Baker, R. C.; Regenstein, J. M. *J. Food Prot.* **1990**, *53*, 465–470.
(14) Tsai, L. S.; Higby, R.; Schade, J. *J. Agric. Food Chem.* **1995**, *43*, 2768–2773.
(15) Napolitano, M. J.; Green, B. J.; Margerum, D. W. *Chem. Res. Toxicol.* **2005**, *18*, 501–508.
(16) Ison, A.; Odeh, I. N.; Margerum, D. W. *Inorg. Chem.* **2006**, *45*, 8768–8775.
(17) Napolitano, M. J.; Stewart, D. J.; Margerum, D. W. *Chem. Res. Toxicol.* **2006**, *19*, 1451–1458.
(18) Pirie, A. *Biochem. J.* **1971**, *125*, 203–208.
(19) Nakagawa, M.; Watanabe, H.; Kodato, S.; Okajima, H.; Hino, T.; Flippen, J.; Witkop, B. *Proc. Natl. Acad. Sci. U.S.A.* **1977**, *74*, 4730–4733.

10.1021/ic701761p CCC: $40.75 © 2008 American Chemical Society
Published on Web 02/07/2008

trochemical oxidation,[28] ozonolysis,[29,30] and metal-catalyzed oxidation.[31,32] Trp has been oxidized with numerous one-electron oxidants such as $Br_2^{\bullet-}$,[33,34] $I_2^{\bullet-}$,[33] $(SCN)_2^{\bullet-}$,[33] $CO_3^{\bullet-}$,[33,34] $N_3^{\bullet}$,[34,35] $OH^{\bullet}$,[34] $CCl_3O_2^{\bullet-}$,[36] and $ClO_2^{\bullet}$.[34,37] Also, $^1O_2$ reactions mediated by the photosensitizer Rose Bengal will oxidize Trp.[22] Most one-electron oxidants have been shown to generate the tryptophyl radical cation. The pK_a of this radical cation ($Trp^{\bullet+}$) has been determined to be 4.3.[33]

Pulse radiolysis studies by Shen et al.[34] show that one-electron oxidants such as $OH^{\bullet}$, $N_3^{\bullet}$, $Br_2^{\bullet-}$, and $CO_3^{\bullet-}$ react with Trp and a variety of indoles at near diffusion-controlled rates, with rate constants from 10^8 to 10^{10} M^{-1} s^{-1}. On the other hand, rate constants for the reaction of $ClO_2^{\bullet}$ with various types of indoles (excluding Trp) range from 10^3 to 10^8 M^{-1} s^{-1}. They determined the second-order rate constant for the reaction of $ClO_2^{\bullet}$ with indole to be 1.2×10^4 M^{-1} s^{-1}.

The reactions between indole systems (including Trp) and $ClO_2^{\bullet}$ have been studied by Merényi et al.,[37] who reported that Trp reacts more slowly than related indoles with $ClO_2^{\bullet}$. They also showed that chlorite suppresses the reaction and that 2 mol of $ClO_2^{\bullet}$ are consumed during the oxidation of Trp. On the other hand, a recent study by Ogata[38] reports that 2.8 mol of $ClO_2^{\bullet}$ are consumed per 1 mol of Trp. Our data show that only 2.0 mol of $ClO_2^{\bullet}$ react per 1 mol of Trp, in agreement with those of Merényi et al.[37] Except for the formation of *N*-formylkynurenine (NFK),[38] little has been known about the intermediates and final oxidation products of the Trp/$ClO_2^{\bullet}$ reaction.

The $E°$ value for the $Trp^{\bullet+}$/Trp reduction couple has been determined to be 1.21 V.[37,39–41] Pulse radiolysis experiments have shown that the tryptophyl radical can oxidize ClO_2^- to $ClO_2^{\bullet}$.[39] NFK (Scheme 1) is a commonly reported product that results from photosensitized oxygenation,[18–20,23,42] one-electron oxidants such as $CCl_3O_2^{\bullet}$[36] and $O_2^{\bullet-}$,[43] singlet oxygen,[21] electrochemical oxidation,[28] hydroxylation,[44] ozonolysis,[29] metal-catalyzed oxidation,[31] peroxy-type oxidants,[25,27,32] and very recently $ClO_2^{\bullet}$ oxidation.[38]

Scheme 1. Structures of Species and Their MWs

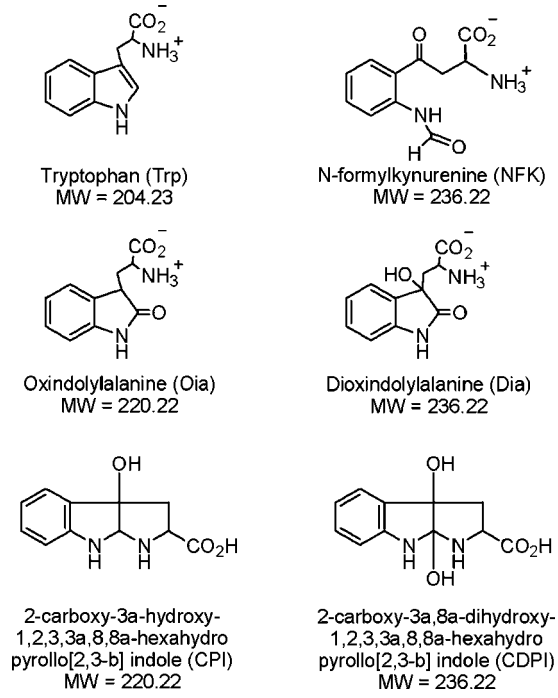

Other reported products of Trp oxidation (shown in Scheme 1) depend on the oxidation methods used. For example, oxindolylalanine (Oia) and dioxindolylalanine (Dia) are formed from photosensitized oxygenation,[20] one-electron oxidation,[43] electrochemical oxidation,[28] hydroxylation,[44] and peroxy-type oxidants.[27] A ring-closure oxidation product of Trp, 2-carboxy-3a-hydroxy-1,2,3,3a,8,8a-hexahydropyrollo[2,3-*b*] indole (CPI), is seen from photooxidation,[19] peroxy-type oxidants,[25,27] and electrochemical oxidation.[28] The dihydroxy form of this product, 2-carboxy-3a,8a-dihydroxy-1,2,3,3a,8,8a-hexahydropyrollo[2,3-*b*] indole (CDPI), is also observed by electrochemical oxidation[28] and is believed to form from intracyclization of Dia.

In the present work, we determine the kinetics, mechanism, and major products of the $ClO_2^{\bullet}$ oxidation of Trp as well as the dependence of $ClO_2^{\bullet}$ decay on p[H^+], [Trp], and [ClO_2^-]. A fascinating array of products is observed. At p[H^+] 6.4, five initial products are seen by high-performance liquid chromatography (HPLC) and are characterized by their UV spectra and mass spectroscopy. One of these products decays with a half-life of about 7 min. Other products form and

(20) Savige, W. E. *Aust. J. Chem.* **1971**, *24*, 1285–1293.
(21) Nakagawa, M.; Okajima, H.; Hino, T. *J. Am. Chem. Soc.* **1976**, *98*, 635–637.
(22) Nakagawa, M.; Yoshikawa, K.; Hino, T. *J. Am. Chem. Soc.* **1975**, *97*, 6496–6501.
(23) Nakagawa, M.; Okajima, H.; Hino, T. *J. Am. Chem. Soc.* **1977**, *99*, 4424–4429.
(24) Sen, A. C.; Ueno, N.; Chakrabarti, B. *Photochem. Photobiol.* **1992**, *55*, 753–764.
(25) Savige, W. *Aust. J. Chem.* **1975**, *28*, 2275–2287.
(26) Itakura, K.; Uchida, K.; Kawakishi, S. *Chem. Res. Toxicol.* **1994**, *7*, 185–190.
(27) Simat, T. J.; Steinhart, H. *J. Agric. Food Chem.* **1998**, *46*, 490–498.
(28) Nguyen, N. T.; Wrona, M. Z.; Dryhurst, G. *J. Electroanal. Chem.* **1986**, *199*, 101–126.
(29) Kotiaho, T.; Eberlin, M. N.; Vainiotalo, P.; Kostiainen, R. *J. Am. Soc. Mass Spectrom.* **2000**, *11*, 526–535.
(30) Fujimora, E. *Invest. Opthalmol. Visual Sci.* **1982**, *22*, 402–405.
(31) Finley, E. L.; Dillon, J.; Crouch, R. K.; Schey, K. L. *Protein Sci.* **1998**, *7*, 2391–2397.
(32) Domingues, M. R. M.; Domingues, P.; Reis, A.; Fonseca, C.; Amado, F. M. L.; Ferrer-Correia, A. J. V. *J. Am. Soc. Mass Spectrom.* **2003**, *14*, 406–416.
(33) Posener, M. L.; Adams, G. E.; Wardman, P.; Cundall, R. B. *Trans. Faraday Soc.* **1976**, *72*, 2231–2239.
(34) Shen, X.; Lind, J.; Merényi, G. *J. Phys. Chem.* **1987**, *91*, 4403–4406.
(35) Jovanovic, S. V.; Steenken, S.; Simic, M. G. *J. Phys. Chem.* **1986**, *90*, 1935–1939.
(36) Shen, X.; Lind, J.; Eriksen, T.; Merényi, G. *J. Chem. Soc., Perkin Trans. 2* **1989**, *6*, 555–562.
(37) Merényi, G.; Lind, J.; Shen, X. *J. Phys. Chem.* **1988**, *92*, 134–137.
(38) Ogata, N. *Biochemistry* **2007**, *46*, 4898–4911.
(39) Jovanovic, S. V.; Steenken, S.; Simic, M. G. *J. Phys. Chem.* **1995**, *95*, 684–687.
(40) Jovanovic, S. V.; Steenken, S. *J. Phys. Chem.* **1992**, *96*, 6674–6679.
(41) DeFelippis, M. R.; Murthy, C. P.; Faraggi, M.; Klapper, M. H. *Biochem.* **1989**, *28*, 4847–4853.
(42) Saito, I.; Matsuura, T.; Nakagawa, M.; Hino, T. *Acc. Chem. Res.* **1977**, *10*, 346–352.
(43) Shen, X.; Lind, J.; Eriksen, T.; Merényi, G. *J. Chem. Soc., Perkin Trans. 2* **1990**, *4*, 597–603.
(44) Maskos, Z.; Rush, J. D.; Koppenol, W. H. *Arch. Biochem. Biophys.* **1992**, *296*, 514–520.

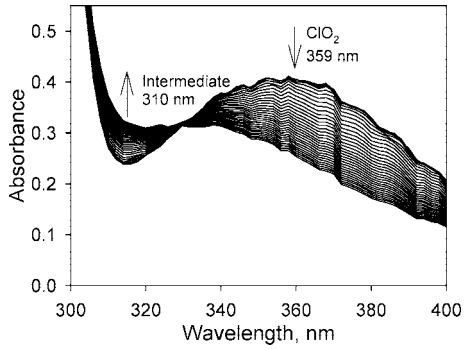

Figure 1. Kinetic spectra for the reaction between $ClO_2^{\bullet}$ and Trp. Individual spectral traces are recorded every 2 nm from 3 to 17 ms. Loss of $ClO_2^{\bullet}$ is seen at 359 nm, and an intermediate forms at 310 nm. Conditions: [Trp] 2.00 mM, $[ClO_2^{\bullet}]$ 0.40 mM, p[H^+] 6.40, $[PO_4]_T$ 20.0 mM, μ = 1.0 M ($NaClO_4$), 25.0 °C, and a path length of 0.962 cm.

decay over a period of 4−72 h to give one major and two minor species.

Experimental Procedures

Reagents. All solutions were prepared with doubly deionized, distilled water. Sodium perchlorate ($NaClO_4$) was recrystallized and standardized gravimetrically prior to use. Tryptophan (Trp; Sigma-Aldrich) was used without further purification. Trp solutions were freshly prepared on the same day as the experiment. $ClO_2^{\bullet}$ was prepared and standardized as previously reported[45] and stored in a dark refrigerator to slow decomposition. Commercially available sodium chlorite ($NaClO_2$) was recrystallized and standardized before use.[46]

Methods. The pH measurements were corrected to give p[H^+] values (=−log [H^+]) based on electrode calibration at 1.0 M ionic strength controlled by the addition of $NaClO_4$.[45]

UV–vis and kinetic spectra were obtained from a Perkin-Elmer Lambda-9 UV–vis−NIR spectrophotometer (1.00 cm path length) or an Applied Photophysics stopped-flow SX.18 MV (APPSF) spectrophotometer (0.962 cm path length) with a PD.1 photodiode-array or single-wavelength detector. Kinetic spectra were obtained either from the photodiode-array detector or by a combination of multiple single-wavelength measurements. Single-wavelength stopped-flow reactions on the APPSF instrument with pseudo-first-order rate constants greater than 80 s^{-1} were corrected for mixing by use of a mixing rate constant of k_{mix} = 4620 s^{-1}, where $k_{corr} = (1/k_{obs} - 1/k_{mix})^{-1}$.[47] Analyses of kinetic data were performed by using Sigma Plot 8.0 or 10.0 software. Many APPSF experiments were performed at 390 nm to follow $ClO_2^{\bullet}$ loss and avoid interference from intermediates and products that absorb at lower wavelengths. The molar absorptivity of $ClO_2^{\bullet}$ at 390 nm was previously reported to be 760(3) M^{-1} cm^{-1}.[17] Fluorescence data were obtained using a Varian Cary-Eclipse spectrophotometer.

Chromatographic analysis was performed with a Varian 5020 HPLC with a Hewlett-Packard 1050 diode-array detector (1.00 cm path length). A Whatman Partisil 5 ODS-3 C_{18} column (250 mm length and 4.6 mm diameter) was used for the reversed-phase liquid chromatography determination of Trp and its oxidized products. Mixtures of 5.0% methanol/0.1% acetic acid and 6.3% methanol/0.1% acetic acid (by volume) were used as eluents in the experiments. The flow rate was 1.0 mL/min. Electrospray ionization

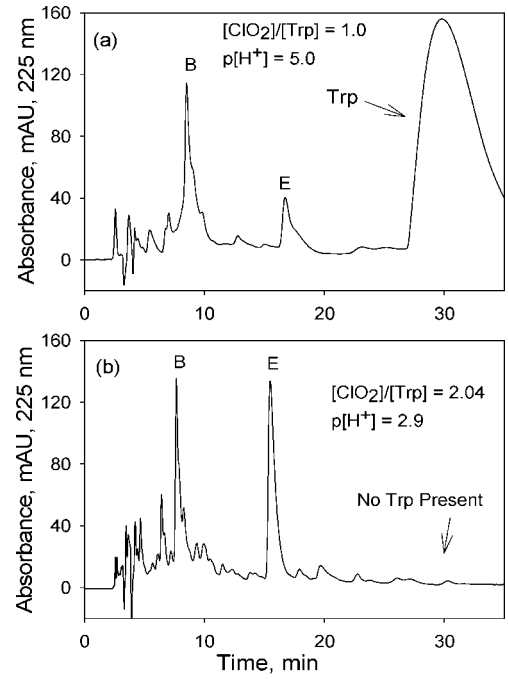

Figure 2. Chromatograms of $ClO_2^{\bullet}$/Trp reactions in different starting molar ratios sampled 5 min after mixing. Reaction conditions: (a) equimolar Trp and $ClO_2^{\bullet}$ (2.0 mM), p[H^+] 5.0, $[OAc]_T$ = 50 mM; (b) excess $ClO_2^{\bullet}$, [Trp] 3.0 mM, $[ClO_2^{\bullet}]$ 6.12 mM, p[H^+] 2.90 (no buffer). HPLC conditions: Whatman Partisil 5 ODS-3 C_{18} column, eluent 5% MeOH and 0.1% acetic acid by volume, 50 μL injection, and λ_{det} = 225 nm.

mass spectrometric (ESI-MS) analyses were carried out in the Purdue Medicinal Chemistry and Molecular Pharmacology Department with a ThermoFinnigan MAT LCQ mass spectrometer system. The electrospray needle voltage was set at 3.5 kV, the heated capillary voltage was set to 23 V, and the capillary temperature was set to 213 °C. Typical background source pressure was 1.2 × 10^{-5} Torr, as read by an ion gauge. The sample flow rate was approximately 8 μL/min. The drying gas was nitrogen. The LCQ was scanned to 600 amu for these experiments.

A Dionex DX-500 chromatograph was used to determine the amounts of ClO_2^- and Cl^- generated from the $ClO_2^{\bullet}$/Trp reaction. Samples were injected by an autosampler (AS 40) through a 25 μL injection loop onto a quaternary amine anion exchange guard (AG9 HC) and separation (AS9 HC) columns. Analytes were eluted with 9 mM Na_2CO_3 with a flow rate of 1 mL/min. Detection of analytes was accomplished by gas-assisted suppressed-conductivity detection (ED 40) with an ASRS-Ultra suppressor in self-regenerating mode and a current of 100 mA.

Results and Discussion

Spectral Observations of the $ClO_2^{\bullet}$ Reaction with Trp. The reaction of $ClO_2^{\bullet}$ with Trp was studied from p[H^+] 3 to 10 by stopped-flow methods with photodiode-array or single-wavelength detection. A kinetic spectrum composed of single-wavelength traces from 3 to 17 ms recorded every 2 nm from 300 to 400 nm is shown in Figure 1 for the reaction of $ClO_2^{\bullet}$ (0.4 mM) with Trp (2.0 mM) at p[H^+] 6.4. The large increase in absorbance below 305 nm is due to excess Trp in the reaction mixture. Spectral changes occur in less than 20 ms, with $ClO_2^{\bullet}$ loss observed at 359 nm and intermediate formation observed at 310 nm. The decay of

(45) Furman, C. S.; Margerum, D. W. *Inorg. Chem.* **1998**, *37*, 4321–4327.
(46) Jia, Z.; Margerum, D. W.; Francisco, J. S. *Inorg. Chem.* **2000**, *39*, 2614–2620.
(47) Nicoson, J. S.; Margerum, D. W. *Inorg. Chem.* **2002**, *41*, 342–347.

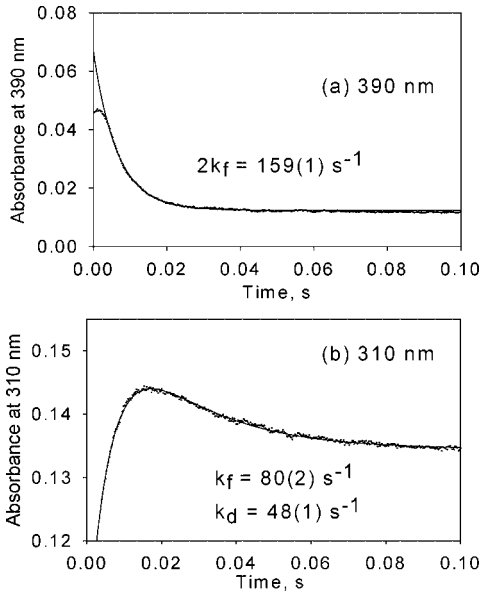

Figure 3. Kinetic traces of $ClO_2^{\bullet}$ decay (a) and of intermediate growth and decay (b). Traces were obtained by APPSF spectrophotometer using single-wavelength detection. Each trace is the average of five pushes. Conditions: [Trp] 2.00 mM, $[ClO_2^{\bullet}]$ 0.10 mM, p[H^+] 7.10, $[PO_4]_T$ 40.0 mM, μ = 1.0 M ($NaClO_4$), 25 °C, (a) λ = 390 nm and (b) λ = 310 nm, and a path length of 0.962 cm.

$ClO_2^{\bullet}$ and formation of the intermediate are concurrent with an observed isobestic point at 330 nm.

Longer term spectral observations were investigated by using a UV–vis spectrophotometer. Spectra were obtained from scans every 2 min over a 90 min period for the reaction of $ClO_2^{\bullet}$ (1.0 mM) with Trp (0.5 mM) at p[H^+] 6.18 (Figure S1 in the Supporting Information). An increase in absorbance at 320 and 265 nm is attributed to the formation of NFK) as shown in Scheme 1, which has absorbance maxima at 320 and 260 nm.

Reaction Stoichiometry. The reaction stoichiometry was determined by measuring the amount of Trp remaining in HPLC experiments as the $ClO_2^{\bullet}$/Trp ratio was varied (Figure 2). When the $ClO_2^{\bullet}$/Trp ratio is below 2:1, Trp absorbance is seen at an elution time of about 30 min. However, the Trp absorbance disappears completely when the ratio is increased to slightly greater than 2:1. Figure 3a shows the rapid decrease in absorbance at 390 nm due to $ClO_2^{\bullet}$ loss, and Figure 3b shows the buildup and decay of an intermediate Trp–OClO species at 310 nm. The rate constant for $ClO_2^{\bullet}$ loss is twice the value of the rate constant for intermediate formation (k_f). This shows that two $ClO_2^{\bullet}$ molecules are needed to form the proposed Trp–OClO adduct and supports the 2:1 $ClO_2^{\bullet}$/Trp stoichiometry. The stoichiometry of the reaction between $ClO_2^{\bullet}$ and Trp is given in a simplified mechanism (p[H^+] < 7) in eqs 1−4, where Trp is in a zwitterion form. This stoichiometry also has been observed by Merényi et al. for the overall reaction.[37]

$$\mathrm{Trp} + \mathrm{ClO_2^{\bullet}} \rightleftarrows \mathrm{Trp^{\bullet+}} + \mathrm{ClO_2^-} \quad k_1/k_{-1} \tag{1}$$

$$\mathrm{Trp^{\bullet+}} \rightleftarrows \mathrm{Trp^{\bullet}} + \mathrm{H^+} \quad K_{a2} = 10^{-4.3} \tag{2}$$

$$\mathrm{Trp^{\bullet}} + \mathrm{ClO_2^{\bullet}} \rightarrow \mathrm{Trp{-}OClO} \quad k_3 \tag{3}$$

$$\mathrm{Trp{-}OClO} \rightarrow \mathrm{products{+}HOCl} \quad k_4 \tag{4}$$

Equation 1 shows an electron transfer from the Trp zwitterion to $ClO_2^{\bullet}$ to produce a radical cation $Trp^{\bullet+}$ and chlorite ion. Equation 2 shows the deprotonation of the indole NH group of the radical cation with a value of $10^{-4.3}$ for K_{a2}.[33] This is followed by the addition of a second molecule of $ClO_2^{\bullet}$ in eq 3 to form a Trp/OClO adduct. This adduct decays (eq 4) to form products and HOCl.

We see a 2:1 $ClO_2^{\bullet}$/Trp stoichiometry in agreement with that of Merényi et al.[37] Although a recent paper by Ogata[38] reported a 2.8:1 stoichiometry, he used excess $ClO_2^{\bullet}$ for all of his stoichiometric determinations. Because of the strong oxidizing capability of $ClO_2^{\bullet}$, the excess $ClO_2^{\bullet}$ in the reaction mixture will almost certainly react with the initially formed products to generate even more highly oxidized products, thus decreasing the amount of $ClO_2^{\bullet}$ remaining to be measured. We observe a rate constant for $ClO_2^{\bullet}$ loss that is twice as large as the intermediate formation (Figure 3), and we show that all of Trp disappears when the reaction stoichiometry is increased to slightly greater than 2:1 (Figure 2). This confirms an actual reaction stoichiometry of 2 $ClO_2^{\bullet}$ per 1 Trp.

The inorganic products generated from the reaction are measured by ion chromatography (IC; Table 1). The results show that, for $ClO_2^{\bullet}$ concentrations from 0.1 to 1.0 mM, the corresponding ClO_2^- concentrations are approximately half the initial $ClO_2^{\bullet}$ concentrations ($[ClO_2^{\bullet}]_i$), in agreement with a 2:1 $ClO_2^{\bullet}$/Trp stoichiometry. A chloride ion also is observed in the IC experiments at approximately half $[ClO_2^{\bullet}]_i$ because HOCl reacts with the IC column to form Cl^-. Previous studies of $ClO_2^{\bullet}$/amino acid reactions[15,16] have shown that HOCl is generated via a four-electron oxidation. Therefore, it is difficult to distinguish whether the Cl^- observed by IC is formed from HOCl/Trp oxidations or from the HOCl reaction with the IC column. The ratio of $([ClO_2^-] + [Cl^-])/[ClO_2^{\bullet}]_i$ is approximately equal to one, and therefore chlorinated Trp products must not be formed. Also, there is no evidence of chlorination in the MS spectra such as Cl 3:1 doublets.

Kinetic Analysis of ClO_2 Loss and Intermediate Formation. A first-order rate of $ClO_2^{\bullet}$ loss (eq 5) is observed when a 10-fold excess of Trp is present above p[H^+] 5.0.

$$-\frac{\mathrm{d}[\mathrm{ClO_2^{\bullet}}]}{\mathrm{d}t} = k_{\mathrm{obs}}[\mathrm{ClO_2^{\bullet}}] \tag{5}$$

Table 1. IC Measurements of Chlorite and Chloride Formation in the Reaction of $ClO_2^{\bullet}$ with Trp[a]

added	found			
$[ClO_2^{\bullet}]_i$, mM	$[ClO_2^-]$, mM	$[ClO_2^-]/[ClO_2^{\bullet}]_i$	$[Cl^-]$, mM	$[Cl^-]/[ClO_2]_i$
0.10	0.054	0.54	0.064	0.64
0.40	0.21	0.53	0.21	0.54
0.70	0.35	0.50	0.35	0.50
1.00	0.47	0.47	0.45	0.45

[a] Conditions: [Trp] 1.0 mM, p[H^+] 7.0, $[PO_4]_T$ 10 mM, 25 °C, eluent = 9.0 mM Na_2CO_3, and flow rate 1.0 mL/min.

Scheme 2. Proposed Mechanism for the Formation of the Trp/OClO Adduct from the Reaction between $ClO_2^{\bullet}$ and Trp

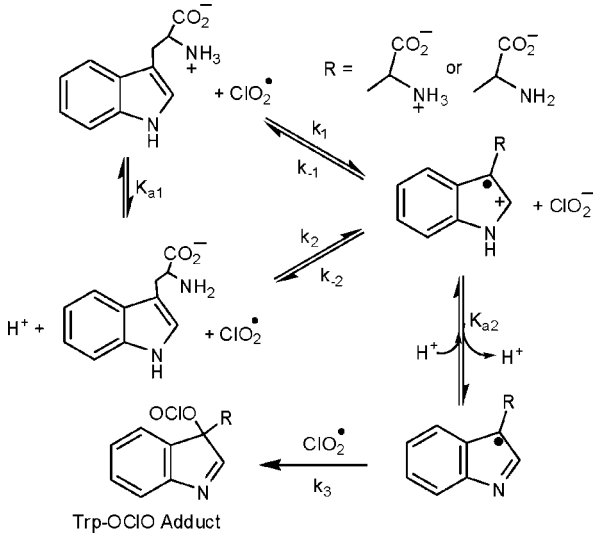

The proposed mechanism from the starting materials to the Trp–OClO adduct is given in Scheme 2 with assigned rate constants. Plots of k_{obs} values for pseudo-first-order loss of $ClO_2^{\bullet}$ as a function of p[H^+] and [Trp] are shown in Figures 4a and 5. Figure 5 shows a linear dependence of k_{obs} on [Trp] at p[H^+] 6.08 and supports a first-order dependence of the reaction on the Trp concentration. The large observed rate constants above p[H^+] 7 are corrected for mixing in the stopped-flow instrument.[47] The rate constants from p[H^+] 5.0–7.0 are relatively constant, while the values above p[H^+] 7 increase rapidly, similar to the results reported by Merényi et al.[37] The plot in Figure 4a of k_{obs} as a function of p[H^+] is fit to eq 6. The experimental pK_{a1} value 9.2 agrees with the pK_a value of 9.3[48] for the ammonium group. As the pH nears 9.3, the Trp zwitterion begins to disappear and Trp takes on a net negative charge. The large increase in the rate constant as the p[H^+] increases is attributed to the electrostatic interaction between the indole ring and the side chain. When $ClO_2^{\bullet}$ extracts an electron from Trp, the positive charge formed on the indole ring and the positive charge on the ammonium group are in close enough proximity to make the reaction approximately 1 order of magnitude less favorable at neutral pH than at high pH, where the ammonium group is deprotonated.

$$k_{obs} = 2k_1[\mathrm{Trp}] + \frac{2k_2K_{a1}[\mathrm{Trp}]_T}{10^{-pK_{a1}} + 10^{-p[H^+]}} \qquad (6)$$

From p[H^+] 3.2 to 4.0 (Figure 4b), the observed rate constants are second-order in [$ClO_2^{\bullet}$] and increase with pH. From p[H^+] 4.0 to 5.0, the kinetic traces do not fit either a first-order or a second-order dependence in [$ClO_2^{\bullet}$], but it is clear that the rate increases as the p[H^+] increases. However, when chlorite is added in excess, the traces become purely second-order depending on p[H^+] and the amount of excess ClO_2^-. Plots of k_{obs} for second-order loss of $ClO_2^{\bullet}$ are shown as functions of 1/[ClO_2^-] (Figure 6). The k_{obs} values have a

(48) Martell, A. E.; Smith, R. M. *Critical Stability Constants. Volume 1: Amino Acids*; Plenum Press: New York, 1974; p 63.

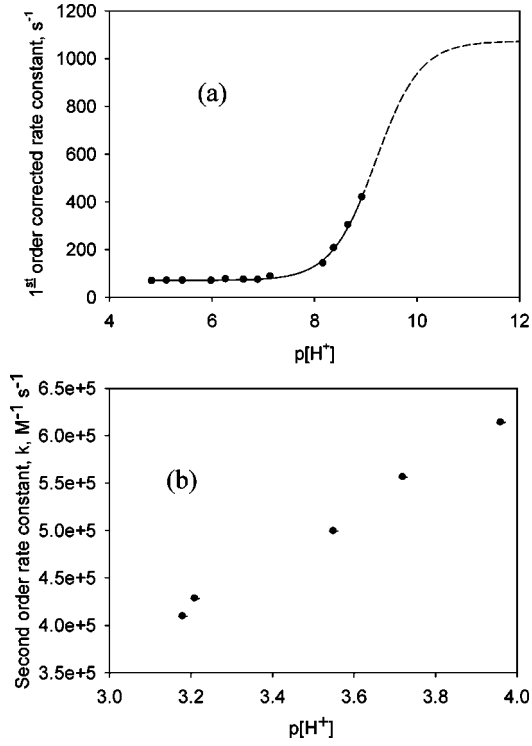

Figure 4. (a) Corrected first-order rate constants for the loss of $ClO_2^{\bullet}$ vs p[H^+]. Conditions: $[Trp]_T$ 1.00 mM, [$ClO_2^{\bullet}$] 0.10 mM, $[PO_4]_T$ 25.0 mM when p[H^+] < 8, $[CO_3]_T$ 50.0 mM when p[H^+] > 8, μ = 1.0 M ($NaClO_4$), 25.0 °C. The curve above p[H^+] 9.0 is the predicted behavior from eq 6. (b) Observed second-order rate constants for the loss of $ClO_2^{\bullet}$ vs p[H^+]. Conditions: $[Trp]_T$ 1.00 mM, [$ClO_2^{\bullet}$] 0.10 mM, $[formate]_T$ 25.0 mM, μ = 1.0 M ($NaClO_4$), 25.0 °C.

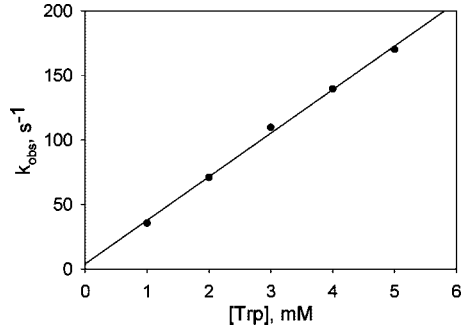

Figure 5. k_{obs} vs [Trp] for the reaction of $ClO_2^{\bullet}$. Conditions: [$ClO_2^{\bullet}$] 0.20 mM, p[H^+] 6.08, $[PO_4]_T$ 100.0 mM, μ = 1.0 M ($NaClO_4$), 25.0 °C, λ = 390 nm. Slope = 3.4(1) × 10^4 M^{-1} s^{-1}.

1/[ClO_2^-] dependence at both p[H^+] 3.60 (Figure 6a) and 6.41 (Figure 6b).

Two rate equations are generated by using the conditions of p[H^+] <5.0 and >5.0. All rate equations assume that $Trp^{\bullet+}$ and $Trp^{\bullet}$ are steady-state species in rapid equilibrium. When p[H^+] is less than 5.0, the deprotonation of the ammonium group is negligible and the k_2/k_{-2} step in Scheme 2 can be omitted. Low p[H^+] will cause the K_{a2} step to be suppressed by [H^+] (pK_a = 4.3[33]) and shift the rate-determining step to k_3. On the basis of the above-mentioned conditions, the rate equation is given in eq 7. The rate expression can be simplified under the conditions used to study the reaction. If [ClO_2^-] is high and/or p[H^+] is low, then k_{-1}[ClO_2^-][H^+] is much larger than k_3K_{a2}[$ClO_2^{\bullet}$] in the denominator of eq 7

and the observed rate expression can be fit to eq 8, consistent with our observations.

$$-\frac{d[ClO_2^{\bullet}]}{dt} = \frac{2k_1k_3K_{a2}[Trp][ClO_2^{\bullet}]^2}{k_{-1}[ClO_2^{-}][H^+] + k_3K_{a2}[ClO_2^{\bullet}]} \quad (7)$$

$$-\frac{d[ClO_2^{\bullet}]}{dt} = \frac{2k_1k_3K_{a2}[Trp][ClO_2^{\bullet}]^2}{k_{-1}[ClO_2^{-}][H^+]} \quad (8)$$

As p[H$^+$] is increased above 5.0 and approaches the pK_{a1} of the ammonium group, [Trp]$_T$ = [Trp] + [Trp$^-$], where [Trp$^-$] is Trp that lost a proton from the ammonium group. As long as no chlorite is added and p[H$^+$] > 5.0, then [Trp$^{\bullet}$] >> [Trp$^{\bullet+}$] and the k_3 step is much faster than the rate-determining step, k_1. In this case, the rate expression is shown in eq 9. The second term in eq 9 is negligible below p[H$^+$] 7 because [H$^+$] is much larger than K_{a1}, but this term is appreciable above p[H$^+$] 7 and accounts for the large increase in the observed rate constant above p[H$^+$] 8 (Figure 4). Values of the rate and equilibrium constants are given in Table 2.

$$-\frac{d[ClO_2^{\bullet}]}{dt} = 2k_1[Trp]_T[ClO_2^{\bullet}] + \frac{2k_2K_{a1}[Trp]_T[ClO_2^{\bullet}]}{[H^+]} \quad (9)$$

Analysis of the $ClO_2^{\bullet}$/Trp Reaction Products. Chromatographic (HPLC) analysis of samples taken 2 min after mixing at p[H$^+$] 6.4 shows seven products (observed at 260 nm). These products have elution times of 2.9 min for HOCl, 3.1 min for ClO_2^-, and 4.5 min (A), 8.7 min (B), 11.9 min (C), 12.6 min (D), and 15.4 min (E) for an eluent mixture of 6.3% methanol/0.1% acetic acid (Figure 7). When the reaction mixture is injected 2 min after mixing, B−D are at their observed maxima while A and E are at relatively low levels (Figure 7a). As the time between mixing and injection lengthens to 62 min, B disappears and C and D decrease while A and E increase (Figure 7b). The ClO_2^- peak height does not change with time, but the HOCl peak decreases with time as species A forms. As shown in Table 3, A and E are the only "stable" products other than ClO_2^-. The amount of species A increases from 62 to 182 min as B is lost, both C and D decay, and a small amount of another product, F, forms. After 362 min, A starts to decay and is nearly gone in 72 h while another species, G, forms (Figure 7c−f). When Trp is used in excess (9.5% over stoichiometric amount) to ensure that all $ClO_2^{\bullet}$ is consumed, it elutes after the products and remains constant with time. HOCl forms from the reaction in eq 4 and is slowly consumed in about 4 h. The ClO_2^- concentration formed (0.92 mM) is determined from the peak area and is approximately half of the initial concentration of $ClO_2^{\bullet}$ (1.95 mM; Figure 7). This agrees with a 2:1 $ClO_2^{\bullet}$/Trp stoichiometry.

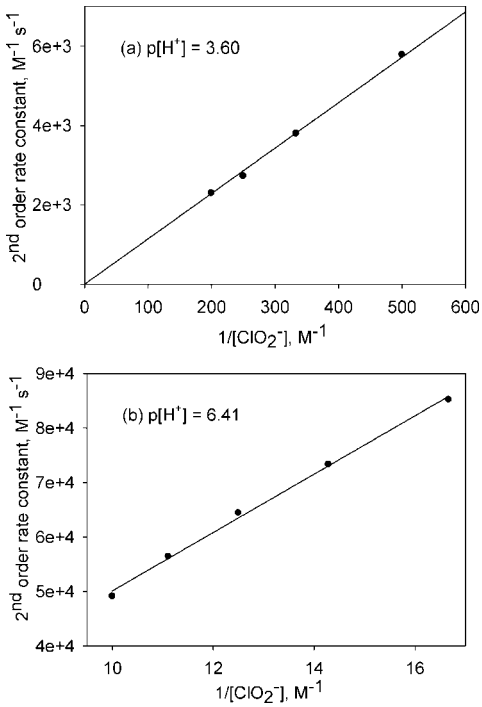

Figure 6. Second-order rate constants vs 1/[ClO_2^-] for the reaction between $ClO_2^{\bullet}$ and excess Trp. Conditions: [Trp] 1.00 mM, [$ClO_2^{\bullet}$] 0.10 mM, μ = 1.0 M ($NaClO_4$), 25.0 °C, λ = 390 nm. (a) [formate]$_T$ 25.0 mM, p[H$^+$] = 3.60, slope = 11.8(4) s^{-1}. (b) [PO_4]$_T$ = 50.0 mM, p[H$^+$] = 6.41, slope = 5.4(2) × 10^3 s^{-1}.

Table 2. Equilibrium and Rate Constants for the Reaction between $ClO_2^{\bullet}$ and Trp as shown in Scheme 2 [a]

constant	value
$E°Trp^{\bullet+}/Trp$ [b]	1.21 V
$E°ClO_2^{\bullet}/ClO_2^-$ [c]	0.934 V
$E°_{rxn}$	−0.276 V
k_1/k_{-1} [d]	2.1 × 10^{-5}
k_1 [e,f]	3.4 × 10^4 M^{-1} s^{-1}
k_{-1}	1.6 × 10^9 M^{-1} s^{-1}
k_3/k_{-1} (av) [e,g]	0.75
k_3 (av) [e,g]	1.2 × 10^9 M^{-1} s^{-1}
k_2 [e,h]	6.3 × 10^5 M^{-1} s^{-1}
K_{a1} [i]	5.0 × 10^{-10} M
K_{a2} [j]	5.0 × 10^{-5} M

[a] Conditions: 25.0 °C. [b] References 37 and 39–41. [c] Reference 51. [d] Calculated from the Nernst equation. [e] Conditions: μ = 1.0 M ($NaClO_4$), present work. [f] Calculated from Figure 5. [g] Calculated by averaging the slopes in parts a and b of Figure 6. [h] Calculated from Figure 4. [i] From ref 48. [j] From ref 33.

All products were observed spectrophotometrically as they eluted (Figure 8 and Figure S3 in the Supporting Information). Product E has a highly characteristic UV–vis spectrum with distinct λ_{max} values at 230, 260, and 320 nm (Figure 8) that exactly match the λ_{max} values for NFK.[20,23,28,49] The ratios of the experimental peak heights of E from 320:260:230 nm are 3.5:10:20, in general agreement with the ratios of 3:10:20 reported for NFK.[23] UV–vis spectral properties of the other products are given in Table 3.

ESI-MS experiments show products B and E ([M + H]$^+$ *m/z* 237) have 32 more mass units than Trp ([M + H]$^+$ *m/z* 205). This corresponds to the addition of two O atoms to Trp, which is consistent with the structure of NFK. When the reaction was carried out in a 95% methanol solution, the most abundant peak ([M + H]$^+$ *m/z* 251) was 46 mass units larger than that of Trp and corresponds to the addition of one oxygen and one methoxy group. This agrees with one oxygen added from $ClO_2^{\bullet}$ and another added from the solution, whether it is water or methanol. The ESI-MS results for the other three products were also observed but are more difficult to interpret. The two less stable products, C and D, have *m/z* (M + H)$^+$ values of 207 and 225, respectively. Product A is more stable and its *m/z* (M + H)$^+$ value is 235.

(49) Pileni, M. P.; Walrant, P.; Antus, R. *J. Phys. Chem.* **1976**, *80*, 1804–1809.

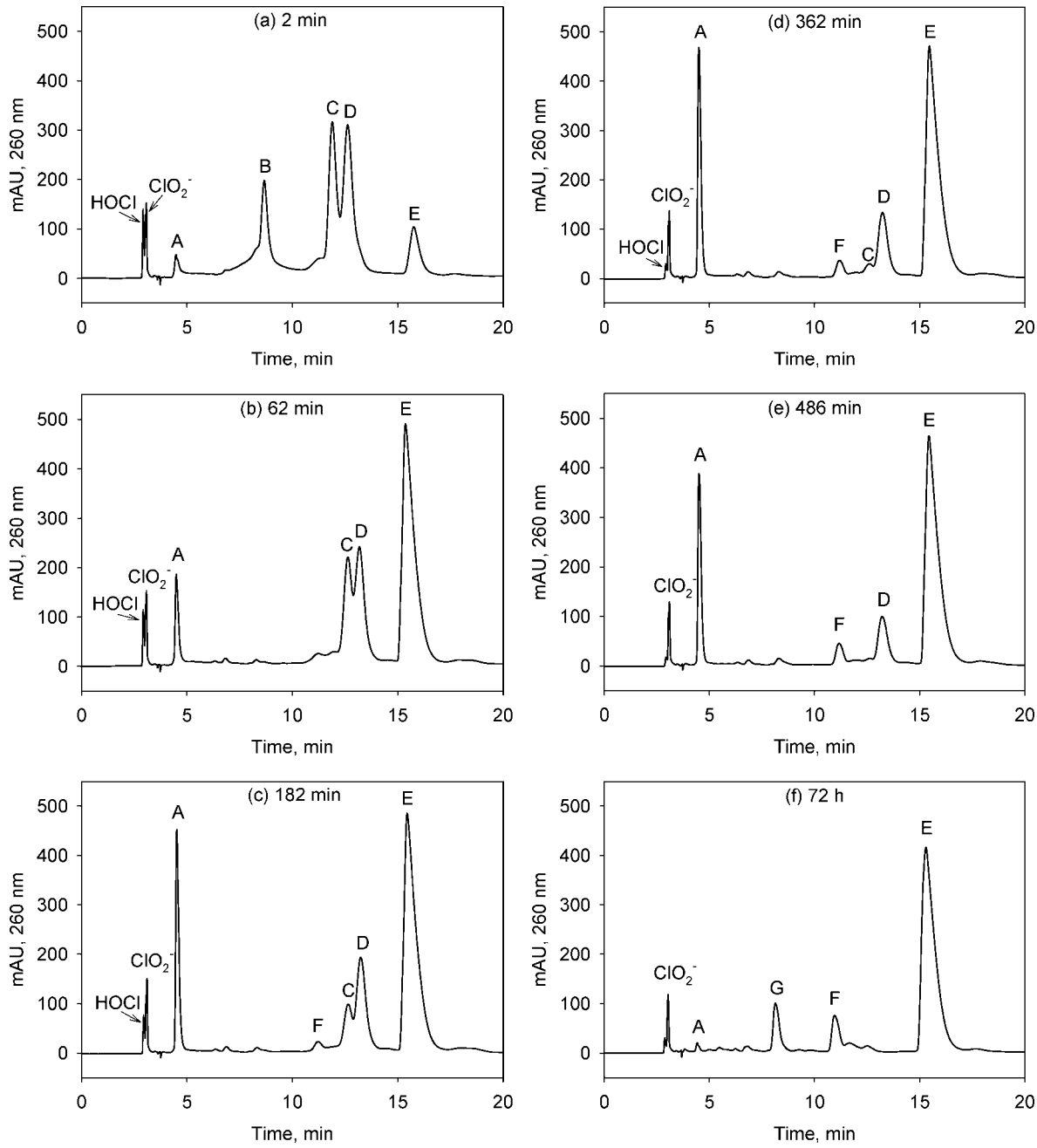

Figure 7. Chromatographs of the products from a mixture of $ClO_2^{\bullet}$ and Trp taken from 2 min (a) to 72 h (f) after mixing. Reaction conditions: [Trp] 1.08 mM, [$ClO_2^{\bullet}$] 1.95 mM, p[H^+] 6.4, $[PO_4]_T$ = 20 mM, 25 °C. HPLC conditions: eluent 6.3% MeOH and 0.1% acetic acid by volume, 100 μL injection, flow rate 1 mL/min, λ_{det} = 260 nm, path length 1.0 cm, Hewlett-Packard 1050 diode-array detector, Whatman Partisil 5 ODS-3 C_{18} column, 250 mm length, 4.6 mm diameter.

Table 3. Chromatographic, UV, and MS Properties of the Observed Products[a]

product	elution time (min)	formation time	50% decay time	absorbance maxima (nm)	*m*/*z* $(M + H)^+$
HOCl	2.9	<1 min	~200 min	216, 274 (sh)	
ClO_2^-	3.1	<1 min	stable	260, 288 (sh)	
A	4.5	~4 h	~920 min	267	235
B	8.7	≤2 min	≤7 min[b]	225, 260 (sh)	237
C	11.9	≤2 min	~100 min	268	207
D	12.6	≤2 min	~240 min	268	225
E (NFK)	15.4	~62 min	stable	230, 260, 320 (w)	237
F	10.9	≥72 h		236, 264, 344 (w)	
G	8.1	~72 h		208, 248, 316 (w), 350 (w)	

[a] Reaction conditions: p[H^+] 6.4, 25.0 °C, eluent 6.3% methanol and 0.1% acetic acid (by volume). [b] Estimated from Figure S4 in the Supporting Information. Reaction conditions: p[H^+] 6.2, 25.0 °C, eluent 5.0% methanol and 0.1% acetic acid (by volume).

The fluorescence spectrum of E in water has a λ_{max} value from 440 to 450 nm when excited at 260 nm (Figure 9). This is close to the λ_{max} value (430 nm) of a species similar to NFK.[49] The derivative used in their work[49] had a methyl

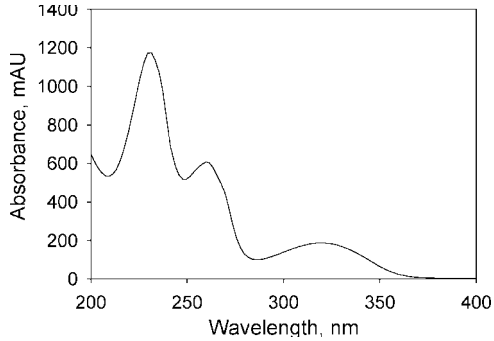

Figure 8. Absorption spectrum of product E from HPLC separation. Path length 1.0 cm.

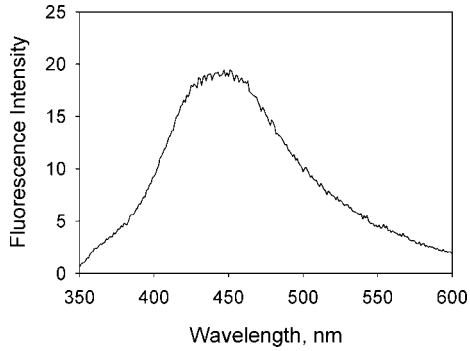

Figure 9. Emission spectrum of product E in water under excitation at 260 nm. E was collected from HPLC elution, freeze-dried, and then dissolved in water for fluorescence analysis.

Scheme 3. Proposed Mechanism from the Trp/OClO Adduct to NFK (Product E)

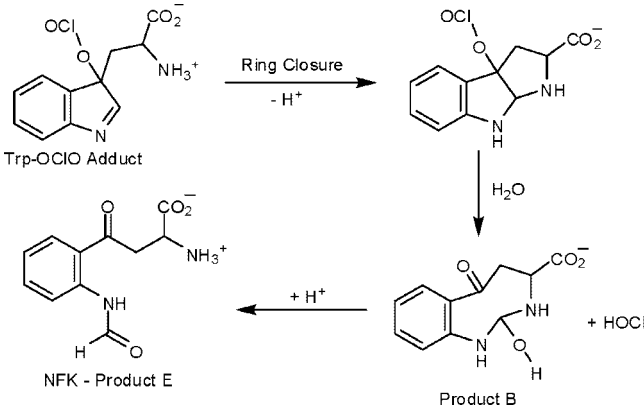

group in place of the amino acid backbone that NFK contains. This slight structural difference may cause λ_{max} shift from 430 to 445 nm.

A very interesting part of this product analysis is that we see a wide variety of species that form: some short-lived and others as more stable products. Although we have not identified all of the products, we can assign NFK as product E based on its mass, UV–vis spectral characteristics, and stability. Product B is proposed as an intermediate to NFK (Scheme 3) because B decays as E forms. The proposed product has the correct mass and follows a ring-closure pathway similar to that in previous work.[28] We observe another relatively stable product with a molecular weight (MW) of 234 (product A). This could form by an HOCl oxidation of NFK to form a product with MW = 234. This is proposed in Scheme 4, with an isocyanate species being

Scheme 4. Possible Pathway to Product A (MW = 234)

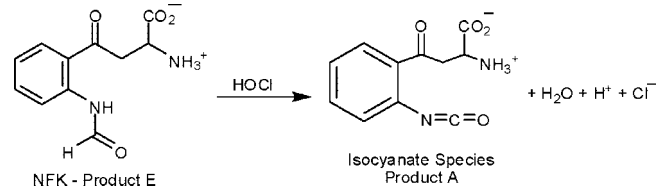

assigned for product A, similar to a previously studied species.[50] While the loss of NFK in Figure 7c appears small compared to the growth of A, it is important to note that the wavelength used is at the maximum of A but not E. Also, the molar absorptivity of A could be large compared to that of E at this wavelength. Some A could also be formed in other pathways by the decay of intermediate products C and D. However, the MWs of products C and D do not correspond to any obvious structures and remain unassigned. The amount of NFK formed is determined from the peak area from Figure 7b and the molar absorptivity (10 980 M^{-1} cm^{-1}) at 260 nm.[18] We find that 31% of the initial Trp is converted to NFK and therefore assign 69% to other products.

Mechanism of the ClO_2/Trp Reaction. The overall proposed mechanism for the $ClO_2^{\bullet}$/Trp reaction to NFK is shown in Schemes 2 and 3 and eq 10. The first $ClO_2^{\bullet}$ molecule reacts with Trp to form a radical cation species ($Trp^{\bullet+}$) and ClO_2^-. This step is reversible and accounts for the inverse [ClO_2^-] dependence on the reaction. The next step is the loss of a proton from the imide group to form a Trp radical ($Trp^{\bullet}$). This step also is reversible with a pK_a of 4.3[33] and accounts for the inverse [H^+] dependence on the reaction. $Trp^{\bullet}$ then reacts with another $ClO_2^{\bullet}$ to form a Trp–OClO adduct, which is an intermediate observed at 310 nm. This step is fast when no chlorite is present at neutral p[H^+] and above but is rate-determining in the presence of high ClO_2^- concentration or low p[H^+]. After the Trp–OClO adduct is formed, it reacts with water (k_d = 48 s^{-1}) to form product B, which rearranges to give product E (NFK). Note that dioxygen is not involved in the reaction.

$$\mathrm{Trp} + 2\mathrm{ClO_2^{\bullet}} + \mathrm{H_2O} \rightarrow \mathrm{NFK} + \mathrm{ClO_2^-} + \mathrm{HOCl} + \mathrm{H^+} \quad (10)$$

Conclusions

Our results show that 2 mol of $ClO_2^{\bullet}$ react with 1 mol of Trp to form ClO_2^- and a Trp–OClO adduct that reacts further to yield several stable products, one of which is NFK. We propose that $ClO_2^{\bullet}$ reacts first by electron transfer to form a $Trp^{\bullet+}$ species, which then reacts with a second $ClO_2^{\bullet}$ molecule by radical–radical bond formation to give a Trp–OClO adduct. This adduct decays with a half-life of about 14 ms. The overall reaction is a four-electron oxidation by two $ClO_2^{\bullet}$, where ClO_2^- and HOCl are the reduction

(50) Green, B. J.; Tesfai, T. M.; Margerum, D. W. *Dalton Trans.* **2004**, *21*, 3508–3514.
(51) Kläning, U. K.; Sehested, K.; Holcman, J. *J. Phys. Chem.* **1985**, *89*, 760–763.

products. After this initial reaction, a series of Trp oxidation products are observed to form and decay over periods of minutes to days.

This study shows that $ClO_2^{\bullet}$ oxidation of Trp is relatively fast at pH 7.0 and 1.0 M ionic strength with a second-order rate constant of $3.4 \times 10^4\ M^{-1}\ s^{-1}$ at 25 °C. The oxidation of Trp by $ClO_2^{\bullet}$ forms several intermediates that then generate NFK and other products. At pH 7.0, the rate of the $ClO_2^{\bullet}$ reaction with Trp is slower than its reaction with tyrosine ($1.3 \times 10^5\ M^{-1}\ s^{-1}$)[15] or cysteine ($6.9 \times 10^6\ M^{-1}\ s^{-1}$)[16] but is much faster than the $ClO_2^{\bullet}$ reaction with guanosine 5′-monophosphate ($4.5 \times 10^2\ M^{-1}\ s^{-1}$).[17]

Acknowledgment. This work was supported in part by National Science Foundation Grant CHE-1039876 and by Purdue University Distinguished Professor Funds for D.W.M.

Supporting Information Available: Kinetic spectra for the reaction of ClO_2 with Trp, HPLC peak area versus time data for products A−D, F, and G, absorption spectra of products A−D, F, and G from HPLC, chromatographs of the ClO_2/Trp mixture, obtained with an eluent mixture of 5.0% methanol/0.1% acetic acid. This material is available free of charge via the Internet at http://pubs.acs.org.

IC701761P